LOW-LEVEL RF SYSTEMS FOR SYNCHROTRONS
Part I: the low-intensity case

P. Baudrenghien
CERN, Geneva, Switzerland

Abstract
The low-level RF system generates the drive sent to the high-power equipment. It uses signals from the main bending magnet (B field) and from beam pick-ups (radial and longitudinal positions). It must minimize the beam losses and provide a beam with reproducible parameters (intensity, bunch length, average momentum and momentum spread) for either the next accelerator or the physicists. This presentation is the first of two: it considers the low intensity case where the voltage in the RF cavity is not influenced by the beam. The feedback loops that do not include the beam (accelerating field amplitude and cavity tuning) will not be presented.

1 BASIC NOTIONS ON ACCELERATION IN SYNCHOTRONS

1.1 The harmonic number

The RF system accelerates particles by producing a time-varying electric field in a cavity. At each turn the particle crosses the cavity. The RF frequency f_{rf} must stay locked in frequency to the revolution frequency f_{rev} otherwise the accelerating voltage will average to zero,

$$f_{rf} = h f_{rev} \ . \tag{1}$$

The integer *h* is called the *harmonic number*.

1.2 The stable phase

At each traversal of the cavity the particle receives an energy kick [1]–[3]

$$\Delta E = qV sin\phi_s \tag{2}$$

where q is the charge of the particle, V is the accelerating voltage and ϕ_s is the phase of the RF when the particle crosses the cavity (synchronous phase or stable phase). The corresponding momentum kick is

$$\Delta p = \frac{\Delta E}{2\pi R_0 f_{rev}} \ , \tag{3}$$

where $2\pi R_0$ is the machine circumference. The rate of change of momentum is thus

$$\frac{dp}{dt} = \Delta p \, f_{rev} = qV sin\phi_s \frac{1}{2\pi R_0} \ . \tag{4}$$

To stay on the centred orbit, the momentum must follow the B field [1]–[3]

$$p = q\rho B \ , \tag{5}$$

where ρ is the bending radius. During acceleration the RF voltage and stable phase will thus obey the relation

$$V sin\phi_s = 2\pi R_0 \rho \frac{dB}{dt} \ . \tag{6}$$

Once the RF voltage is defined, the above relation can be inverted to give the stable phase as a function of the RF voltage and the time derivative of the B field

$$\phi_s = \arcsin\left(2\pi R_0 \rho \frac{\frac{dB}{dt}}{V}\right) \ . \tag{7}$$

The above function is called the stable phase programme (see Fig. 1).

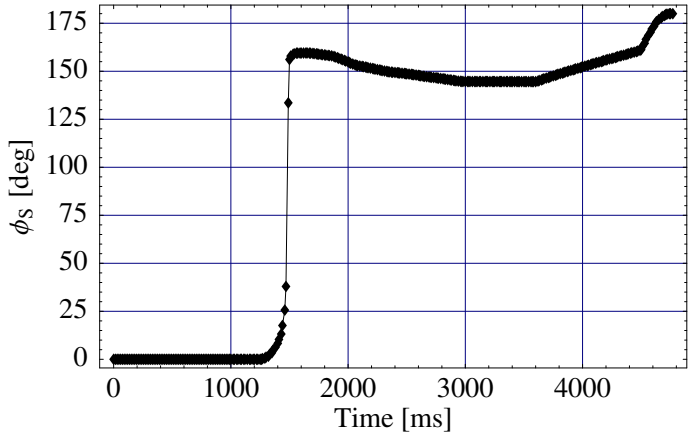

Fig. 1: Variation of the stable phase during the proton cycle in the CERN SPS (acceleration from 14 GeV to 450 GeV). Transition energy (see Section 1.4) at 23 GeV crossed around time 1500 ms with a phase jump from ϕ_s^- to $\phi_s^+ = \pi - \phi_s^-$). Courtesy of T. Bohl, CERN SL/HRF.

1.3 Synchrotron oscillations

By definition the synchronous particle is the particle that stays at the stable phase during the acceleration, i.e. the RF phase when it crosses the cavity is ϕ_s. Its momentum, p_s, is such that it stays on the centre orbit.[1] We define the synchronous RF frequency ω_s as $2\pi h$ times the revolution frequency of the synchronous particle. A bunch consists of many particles. Each particle is characterized by its coordinates in phase and momentum: let $\phi = \phi_s + \delta\phi$ be the phase of the RF when the particle crosses the cavity and let $p = p_s + \delta p$ be its momentum. We now derive the equation of motion in the presence of a small modulation of the RF frequency $\omega_{rf} = \omega_s + \delta\omega_{rf}$. First the momentum gain per turn:

$$\frac{d}{dt}\delta p = \frac{qV}{2\pi R_0}\left(sin(\phi_s + \delta\phi) - sin\phi_s\right) \approx \frac{qV\,cos\,(\phi_s)}{2\pi R_0}\delta\phi \ . \tag{8}$$

The above linear approximation is valid for small phase deviations only. A second equation relates the phase slip to the difference in beam frequency f_b and the RF frequency modulation:

$$\frac{d}{dt}\delta\phi = -2\pi\,\delta f_b + \delta\omega_{rf} \ , \tag{9}$$

where δf_b is the particle frequency deviation that can be related to the momentum deviation via the slippage factor (Eq. 10)[2]

$$\eta = -\frac{\frac{\delta f_b}{f_b}}{\frac{\delta p}{p}} = \frac{1}{\gamma_t^2} - \frac{1}{\gamma^2} \ , \tag{10}$$

[1] The subscript s refers to the synchronous particle.

[2] Some authors define η as $\frac{\frac{\delta f_b}{f_b}}{\frac{\delta p}{p}}$.

where $\gamma = E/E_0$ (E_0 being the rest energy) and γ_t is the value of γ at the transition energy. Recall that $\phi_s + \delta\phi$ is the phase of the RF when the particle crosses the cavity while $f_s + \delta f_b$ is the particle frequency. A faster particle will cross the cavity earlier, i.e. with a negative $\delta\phi$. This explains the minus sign in Eq. (9). By differentiating Eq. (9) and using Eqs. (10) and (8) we get

$$\frac{d^2}{dt^2}\delta\phi + \Omega_s^2\,\delta\phi = \frac{d\delta\omega_{rf}}{dt} \quad . \tag{11}$$

Similarly, by differentiating Eq. (8) and using Eqs. (9) and (82) we get

$$\frac{d^2}{dt^2}\delta p + \Omega_s^2\,\delta p = \frac{qV\,cos\,(\phi_s)}{2\pi R_0}\delta\omega_{rf} \quad . \tag{12}$$

Ω_s is called the synchrotron frequency

$$\Omega_s = \sqrt{-\frac{hqc}{2\pi R_0^2}\frac{\beta_s}{p_s}\eta_s V\,cos\,(\phi_s)} \quad , \tag{13}$$

where β_s is the normalized velocity v_s/c of the synchronous particle. The equation of motion is one of an *undamped resonator excited by the RF frequency noise*. Its resonant frequency Ω_s varies during the acceleration. It depends on the synchronous momentum via the parameters p_s, β_s and γ_s , and on the RF parameters V and ϕ_s. Figure 2 shows a mechanical analogy of the longitudinal motion: an object of mass m is free to move on an horizontal axis. It is subject to the force of a spring of strength k. Let $x(t)$

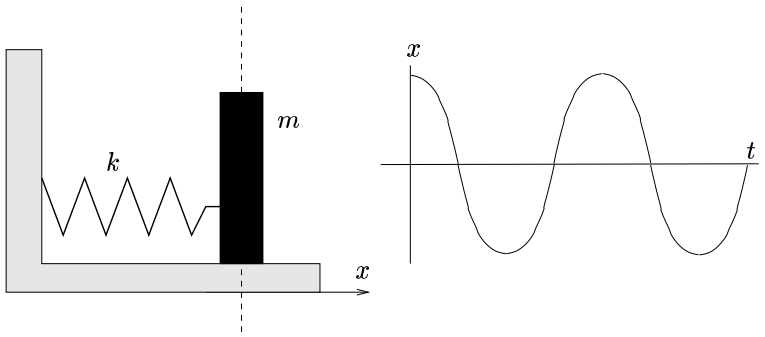

Fig. 2: Mechanical analogy of the synchrotron oscillation

be its position at time t, the equation of motion is

$$\frac{d^2x}{dt^2} + \frac{k}{m}x = 0 \quad . \tag{14}$$

Starting with an initial displacement x_0 and zero velocity, the solution is

$$x(t) = x_0\,cos\,(\Omega t) \tag{15}$$

with $\Omega = \sqrt{\frac{k}{m}}$. The oscillation lasts forever because there is no damping term (first order derivative) in the equation of motion. The motion can also be represented in the $(x,\, \frac{dx}{dt})$ plane, called the phase plane. Since

$$\frac{dx}{dt} = -x_0\Omega\,sin\,(\Omega t) \quad , \tag{16}$$

we have

$$\left(\frac{x}{x_0}\right)^2 + \left(\frac{\frac{dx}{dt}}{x_0\Omega}\right)^2 = 1 \quad . \tag{17}$$

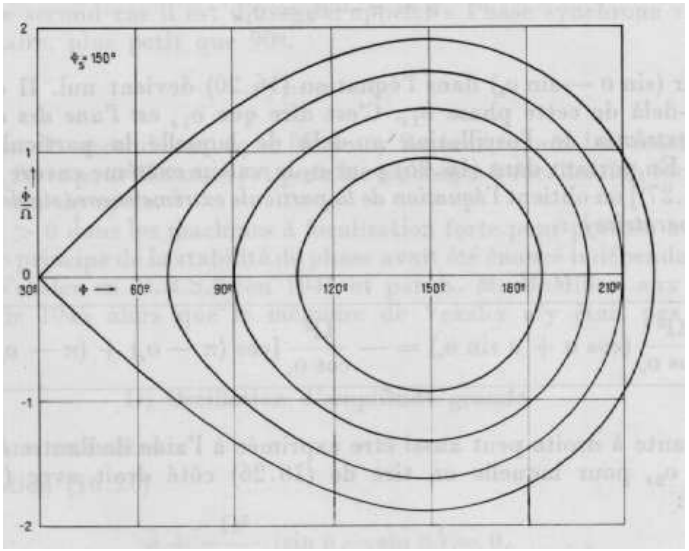

Fig. 3: Phase space trajectory in the $(\phi, \frac{1}{\Omega_s}\frac{d\phi}{dt})$ plane. Case above transition: The particles move clockwise along the trajectories. The stable phase is $150°$. The vertical axis can also be labelled in momentum, energy, frequency or radial position. (Reproduced from Ref. [2]).

The trajectory is an ellipse in phase plane. Similarly the particles that have small phase and momentum deviations with respect to the synchronous particle describe small ellipses around the $(\phi_s, 0)$ point in the $(\phi, \frac{1}{\Omega_s}\frac{d\phi}{dt})$ plane (Fig. 3). As we consider particles with

larger and larger deviations, their trajectory become less elliptic. Recall that we have linearized the equation of motion (8). The largest trajectory shown is called the *separatrix*: its width depends on the stable phase only. In normalized units $\frac{1}{\Omega_s}\frac{d\phi}{dt}$, its height, also depends on the stable phase only. One often uses momentum or energy for the vertical axis. With these units the height of the separatrix is proportional to the square root of the RF voltage [2]. Outside the separatrix the particle trajectories are not closed: These particles are not *captured* by the RF and will be lost as the acceleration proceeds. The area inside the separatrix is called the *RF bucket*. The formula for the synchrotron frequency (13) was derived using the linearized equation of motion. It is exact for small trajectories around the synchronous particle. For larger deviations, the frequency of the oscillation is decreased and finally vanishes on the separatrix [2].

1.4 Transition energy

The slippage factor η is negative at low energy $(\gamma \leq \gamma_t)$ and positive above the transition energy. This change of sign is easily understood: a particle with a momentum in excess (positive $\frac{\delta p}{p}$) will travel faster than the synchronous particle but it will travel on an off-centred orbit since its mass is also larger. Its orbit will thus be longer. At low energy the velocity increase wins over the orbit lengthening and the frequency will increase (negative η). As the energy gets higher, the particle velocity approaches the speed of light and the winning factor is the orbit lengthening (positive η). The equation of motion (11) will be stable only if Ω_s^2 is positive. We thus conclude from Eq. (13) that the sign of $cos\,(\phi_s)$ must change at transition: below transition the particles move counter-clockwise in phase space and $cos\,(\phi_s)$ is positive (ϕ_s will typically be between $0°$ and $30°$). Above transition $cos\,(\phi_s)$ is negative (ϕ_s between $150°$ and $180°$). The phase of the RF must jump at transition as shown in Fig. 1 for the proton cycle in the CERN SPS. Such a critical RF manipulation is possible because the synchrotron frequency goes to zero at transition. The dynamics of the bunch are thus very slow at that critical moment.

1.5 The accelerating bucket

The bunch consists of many particles, each undergoing synchrotron oscillations in phase space. The *longitudinal emittance* of the bunch is the area that it fills in (energy,time) space. It is often measured in eVs. Given the triplet (E_s, V, ϕ_s) we can compute the RF bucket area A in eVs [4]

$$A(E_s, V, \phi_s) = \left(\frac{16\sqrt{e}}{(2\pi)^{\frac{3}{2}}\sqrt{h}}\right) \times \left(\frac{\beta_s\sqrt{E_s}}{f_{rf}\sqrt{|\eta_s|}}\right) \times \left(\sqrt{V}\alpha(\phi_s)\right) \quad . \tag{18}$$

The first factor is constant (if the harmonic number is kept constant). The second factor depends on the energy only. The third factor shows the influence of the RF voltage and the stable phase: $\alpha(\phi)$ is a non-linear function of the stable phase angle. It is equal to one for 0° and 180° (stationary bucket) and drops to 0.3 for 32° or 148° [4]. At injection, the energy spread and bunch length are defined by the injector. We must match the RF bucket to these parameters and this defines the bucket area A_0. From Liouville's theorem we know that the emittance is invariant during acceleration [2]. The bucket area should thus also be kept constant. In practice, however, the RF manipulations will blow up the emittance and we wish to increase the bucket area at some critical points in the cycle (just after transition for example). Once the desired bucket area is defined through the cycle, we can merge Eqs. (18) and (6) to get a system of two equations with two unknowns V and ϕ_s. By solving this we obtain the appropriate values for V (see Fig. 4) and ϕ_s (see Fig. 1) through the acceleration cycle.

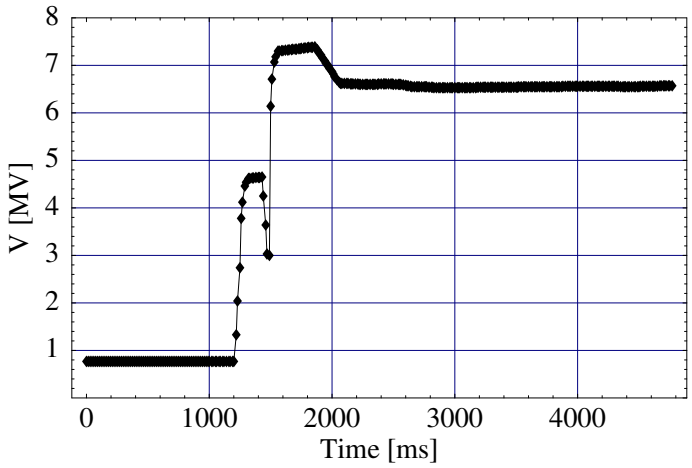

Fig. 4: Variation of the RF voltage during the proton cycle in the CERN SPS (acceleration from 14 GeV to 450 GeV. Transition at 23 GeV). Courtesy of T. Bohl, CERN SL/HRF.

1.6 Bunch transfer function for dipolar motion

In Section 1.3 we examined the motion of a single particle. Let us now consider the bunch as a statistical collection of many particles, each particle oscillating around the synchronous phase. We wish to derive an equation for the motion of the centre of charge of the bunch. Let us freeze the motion at a given instant t and let $f(x)$ be the probability density function for the phase ϕ of the particles. ($f(x)dx$ is the probability that the RF phase be between x and $x + dx$ when the particle crosses the cavity.) The first order moment (centre of charge) $\hat{\phi}$ is

$$\hat{\phi} = \int \phi f(\phi) d\phi \tag{19}$$

where the integration covers the entire bunch. Let $\delta\hat{\phi}$ be $\hat{\phi} - \phi_s$. We have

$$\delta\hat{\phi} = \hat{\phi} - \phi_s = \int \phi f(\phi) d\phi \; - \phi_s \quad . \tag{20}$$

By definition the probability density function integrates to 1

$$\int f(\phi) d\phi = 1 \tag{21}$$

so that Eq. (20) can be rewritten

$$\hat{\delta\phi} = \int (\phi - \phi_s)\, f(\phi) d\phi = \int \delta\phi f(\phi) d\phi \ . \tag{22}$$

Let us now assume a stationary distribution so that $f(x)$ does not depend on t. Taking the second derivative of the above equation we get

$$\frac{d^2\hat{\delta\phi}}{dt^2} = \int \frac{d^2\delta\phi}{dt^2} f(\phi) d\phi \ . \tag{23}$$

Now using the synchrotron equation (11) for each particle in the bunch

$$\frac{d^2\hat{\delta\phi}}{dt^2} = \int \left(-\Omega_s^2\, \delta\phi + \frac{d\delta\omega_{rf}}{dt} \right) f(\phi) d\phi \tag{24}$$

$$\frac{d^2\hat{\delta\phi}}{dt^2} + \Omega_s^2 \int \delta\phi f(\phi) d\phi = \frac{d\delta\omega_{rf}}{dt} \int f(\phi) d\phi \tag{25}$$

$$\frac{d^2\hat{\delta\phi}}{dt^2} + \Omega_s^2\, \hat{\delta\phi} = \frac{d\delta\omega_{rf}}{dt} \ . \tag{26}$$

The above equation is identical to the synchrotron equation describing the motion of each particle. These cannot be individually observed by the instrumentation. On the other hand the motion of the centre of charge of the bunch, also called *dipolar motion*, can easily be monitored.

1.7 The RF frequency

During the acceleration the RF frequency must stay locked to the revolution frequency of the bunch

$$f_{rf} = h f_{rev} = h \frac{v_s}{2\pi R_0} = \frac{hc}{2\pi R_0} \beta_s \tag{27}$$

where the normalized velocity β_s is a function of the momentum p_s

$$\beta_s = \frac{1}{\sqrt{1 + \left(\frac{E_0}{c p_s}\right)^2}} \ . \tag{28}$$

During acceleration the momentum follows the B field according to Eq. (5) and we get

$$f_{rf} = \frac{hc}{2\pi R_0} \frac{B}{\sqrt{B^2 + \left(\frac{1}{c\rho}\frac{E_0}{q}\right)^2}} = f_\infty \sqrt{1 - \frac{1}{\gamma_s^2}} \ , \tag{29}$$

where

$$\gamma_s = \frac{E_s}{E_0} \tag{30}$$

and

$$f_\infty = \frac{hc}{2\pi R_0} \ . \tag{31}$$

The above equation for f_{rf} is called the *frequency programme*. We observe that:

- the RF frequency varies with the energy (or the magnetic field) in a non-linear fashion;
- it can be controlled from a measurement of the magnetic field;
- the frequency swing depends on the range of γ from injection to extraction. For a highly relativistic machine (leptons) where $\gamma \gg 1$, the RF frequency can be kept constant. On the other hand low energy hadron machines need a precise frequency programme. This is also the case for ion acceleration (large $\frac{E_0}{q}$ ratio). Some examples:

  Lepton ($E_0 = 0.511$ MeV) acceleration in the CERN SPS from 3 GeV to 22 GeV at constant frequency 200.395 MHz.

  Proton ($E_0 = 938$ MeV) acceleration in the CERN LHC from 450 GeV (400.789 MHz) to 7 TeV (400.790 MHz).

  Lead ions (208Pb82+) acceleration in the CERN SPS from 5.114 GeV/u (energy per nucleon) at 197.072 MHz to 160 GeV/u (200.393 MHz).

  Original proton acceleration in the CERN PS (1959, h = 20) from 50 MeV (2.9 MHz) to 25 GeV (9.54 MHz) [5];
- the choice of accelerating cavity is dictated by the frequency swing: for a large frequency swing, ferrite cavities are preferred for their important tuning range [6]. For relativistic beams, high Q cavities operated at higher frequencies are the common choice [7].

2 WHY DO WE NEED A LOW-LEVEL SYSTEM?

2.1 The simplest RF system

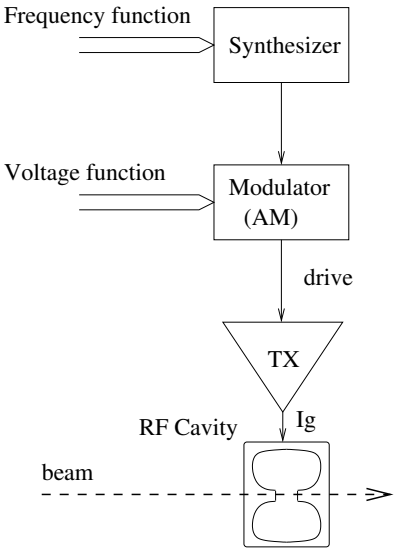

Fig. 5: Simplest RF system. No feedback loop.

The simplest accelerating system for a circular accelerator or collider is shown in Fig. 5. It consists of:

- an accelerating cavity;
- driven by a power amplifier (TX);
- whose drive is adjusted in amplitude by a modulator (to vary the accelerating voltage during the ramp in order to keep the desired bucket area A);
- and whose frequency is controlled by a synthesizer to follow the desired function $f_{rf}(B)$.

2.2 What will go wrong?

In general the performance of the above low-level system will not be good for the following reasons:

- The magnetic field fluctuates, so the RF frequency f_{rf} is not correct. This causes a displacement of the orbit δR given by Eq. (80)
$$\frac{\delta R}{R} = \frac{\gamma^2}{\gamma_t^2 - \gamma^2} \frac{\delta f_{rf}}{f_{rf}} \tag{32}$$
- If the transfer from the injector is of the bunch into bucket type, the parameters of the injected beam will not be perfectly stable: the phase will be slightly wrong and the energy will not be perfectly matched to the magnetic field of the receiving machine (radial position error on the first turn).
- The RF synthesizer injects phase noise that shakes the bunches as is evident from Eq. (26).
- The power amplifiers have ripples at multiples of 50 Hz.
- The gain and phase shift of the power amplifiers may drift.
- The beam current will modify the accelerating voltage (beam loading).
- etc ...

The classic control solution is to use feedback loops measuring the slowly drifting parameters and adjusting the RF settings accordingly.

3 WHAT CAN WE MEASURE?

3.1 The magnetic field

The magnetic field can be measured with a high precision: in the CERN SPS for example it is measured with a precision of 3×10^{-5} T over a range of 2 T.

3.2 The radial position

Three factors limit the precision of single turn measurements of the radial position of the beam:

- The sensitivity to the beam intensity: in the SPS the precision is 0.5 mm for a 1 to 10 range of beam intensity [8]. In the LHC the design precision is 0.1 mm for a 1 to 30 (pilot to nominal) range of beam intensity [9].
- The transverse betatron oscillation: the RF is interested in the *mean* radial position of the beam (that is related to the beam energy). If the beam is not injected on the centred trajectory, it will execute a transverse betatron oscillation that must be filtered out of the part interesting the RF.
- The local orbit distortion: usually we use only one or two radial pick-ups in the RF low-level system. These sample the position at one point in the machine. As a consequence the measurement will differ from the mean radial position in the case of a closed orbit distortion at the pick-up location.

3.3 The beam phase (longitudinal position)

The phase of the beam is defined as *the phase of the Fourier component of the beam current at the RF frequency*. (Note that the beam phase is defined by the beam *current* while the RF phase refers to the *voltage* in the cavity. For a beam at stable phase zero below transition, the beam phase will thus lead the cavity phase by $\pi/2$. Above transition, a beam at stable phase π will lag the cavity phase by $\pi/2$.) If the buckets are not evenly filled around the machine the beam current will have a strong amplitude modulation at the revolution frequency. Its spectrum thus shows side-bands at $f_{rf} \pm n f_{rev}$. These must be filtered out of the beam phase signal to avoid exciting higher order coupled bunch dipole oscillations, ($n \geq 1$), with the phase loop.

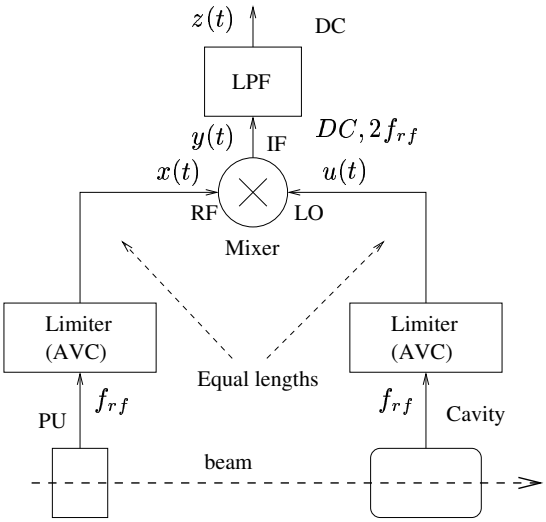

Fig. 6: Direct measurement of the beam/cavity phase. Processing at the RF frequency.

Figure 6 shows a method to measure the phase of the beam with respect to the cavity. The beam signal is generated by a narrow-band pick-up (cavity resonator) centred at the RF frequency. It is followed by a limiter (AVC) that provides a constant RF level at its output so that the phase measurement is insensitive to the beam intensity. The signal from the cavity is processed in an identical chain with an equal delay so that the signals at the input of the mixer stay in phase as the RF frequency varies. Let ϕ_b be the phase of the beam and ϕ_c be the phase of the cavity

$$x(t) = cos(2\pi f_{rf} t + \phi_b) \ , \tag{33}$$

$$u(t) = cos(2\pi f_{rf} t + \phi_c) \ . \tag{34}$$

The mixer multiplies the signals on its RF and LO ports

$$y(t) = cos(2\pi f_{rf} t + \phi_b) cos(2\pi f_{rf} t + \phi_c) = \frac{cos(4\pi f_{rf} t + \phi_b + \phi_c) + cos(\phi_b - \phi_c)}{2} \tag{35}$$

$$z(t) = \frac{cos(\phi_b - \phi_c)}{2} \ . \tag{36}$$

The Low Pass Filter (LPF) must provide a large attenuation at multiples of the revolution frequency. An alternative is to sample its output at the revolution frequency to produce one phase information per turn.

In theory, phase measurements are insensitive to the beam intensity. In practice the phase shift introduced by the limiter in the beam signal path will vary with the level of its input signal. The system of Fig. 6 is used to accelerate the LHC proton beam in the CERN SPS. The frequency swing is only 130 kHz at 200 MHz. Narrow-band limiters have been designed with $\pm 3^\circ$ phase shift for 60 dB input dynamic range in the above frequency range. When the frequency swing is large the system shown in Fig. 7 is preferred. The beam signal from a wide band pick-up (Electrostatic or Wall Current Monitor) is heterodyned to an Intermediate Frequency (IF) and followed by a fixed Band-Pass Filter (BPF) at the IF. For large frequency swings this solution presents the advantage of processing the signal at a fixed intermediate frequency (AGS booster at BNL [10], fixed target beam in the CERN SPS, CERN PS [11]). The LO frequency remains at a fixed frequency offset with respect to the RF during the acceleration: $f_{lo} = f_{rf} - f_{if}$. The BPF at the intermediate frequency selects two bands in the pick-up signal: $f_{lo} + f_{if} = f_{rf}$ and $f_{lo} - f_{if} = f_{rf} - 2f_{if}$. This latter band is called the image. If necessary the noise present in this band can be rejected with the RF BPF. The IF BPF must be narrow enough to reject the sidebands at $f_{rf} \pm n f_{rev}$. (In the CERN SPS we use an IF at 10.7 MHz. The BPF is a 10.7 MHz crystal filter that rejects the 43 kHz side-bands.)

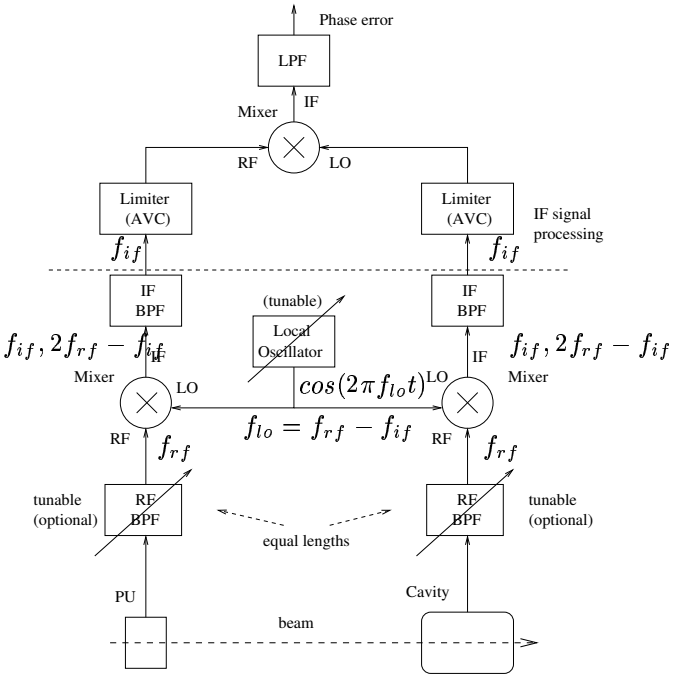

Fig. 7: Heterodyne system for the measurement of the beam/cavity phase. Processing at the IF frequency.

4 WHAT SHOULD BE CONTROLLED?

4.1 Controlling the RF phase seen by the beam: the phase loop

Motivation: The noise in the RF system will excite coherent longitudinal oscillations of the beam. Such an oscillation will also be triggered by a phase or energy error at injection if transfer is of the bunch-into-bucket type. In lepton machines the synchrotron light may provide sufficient natural damping. In hadron machines, however, these oscillations will persist, resulting in emittance blow-up due to filamentation and finally beam loss because the bucket area will be too small. Figure 8 shows a simulation of the injection into the 200 MHz LHC bucket with a small phase and energy error. The spread in synchrotron frequency as a function of the deviation from the synchronous particle causes a *filamentation* of the bunch: the particles with large deviations have smaller synchrotron frequencies and drag behind the core of the bunch. The end result is a severe and often unacceptable blow-up of the emittance.

The cure is easily found if we refer to our mechanical analogy shown in Fig. 2. We must add a friction term (i.e. a force proportional to the velocity as shown in Fig. 9) so that the phase or energy error is quickly damped to zero.

The phase loop is shown in Fig. 10:

The phase of the beam ϕ_b is compared to the phase of the RF in the cavity ϕ_c and the error[3] $\delta\phi_{b,c} = \phi_c - \phi_b + \pi/2 - \phi_s$ is used to correct the frequency of the RF (generated by the Voltage Controlled Oscillator, VCO) via the feedback $\delta\omega_{rf}$. By averaging over the bunches in the beam, Eq. (26) for the synchrotron oscillation of the centre of charge of each bunch transforms into an identical equation for the whole beam

$$\frac{d^2\delta\phi_{b,c}}{dt^2} + \Omega_s^2\,\delta\phi_{b,c} = \frac{d\delta\omega_{rf}}{dt} \quad . \tag{37}$$

We now introduce a feedback term

$$\delta\omega_{rf} = -k_\phi\,\delta\phi_{b,c} \tag{38}$$

[3] The $\pi/2$ term is due to the comparison of the phase of the beam *current* to the phase of the cavity *voltage*. For a beam at stable phase zero below transition, the beam phase will thus lead the cavity phase by $\pi/2$.

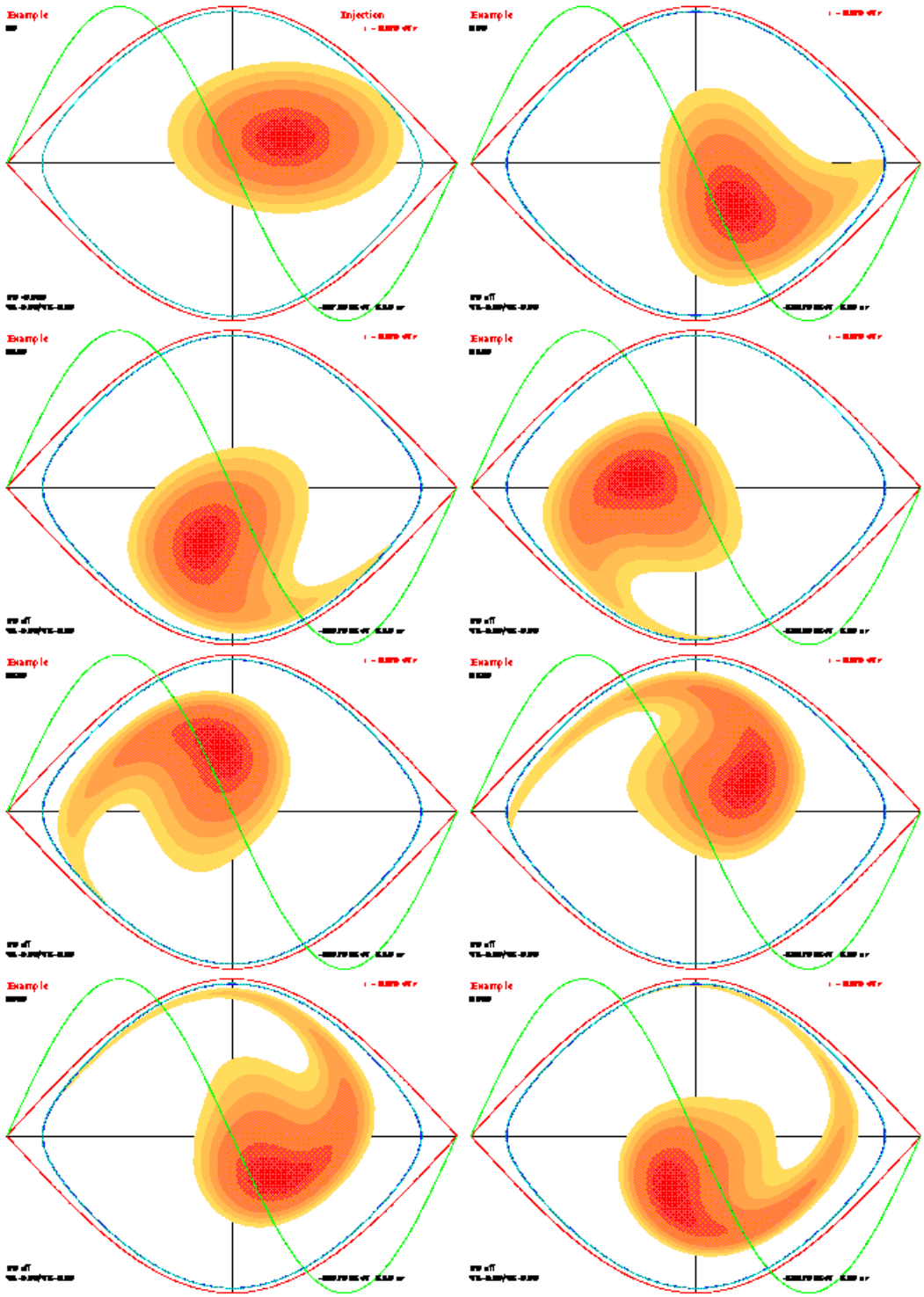

Fig. 8: Phase and energy error at injection into the LHC (450 GeV, 4 MV RF at 200 MHz, $f_{rev} = 11$ kHz). Simulation of the filamentation of the bunch. First turn at top left. Later plots to be read from left to right and from top to bottom. 50 turns between plots. Courtesy of J. Tuckmantel, CERN SL/HRF.

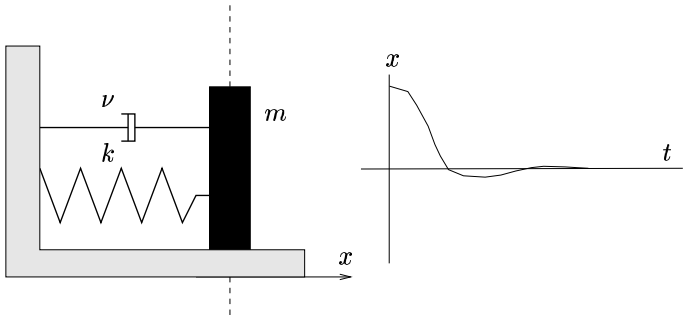

Fig. 9: Damping of our mechanical analogy for the synchrotron oscillation

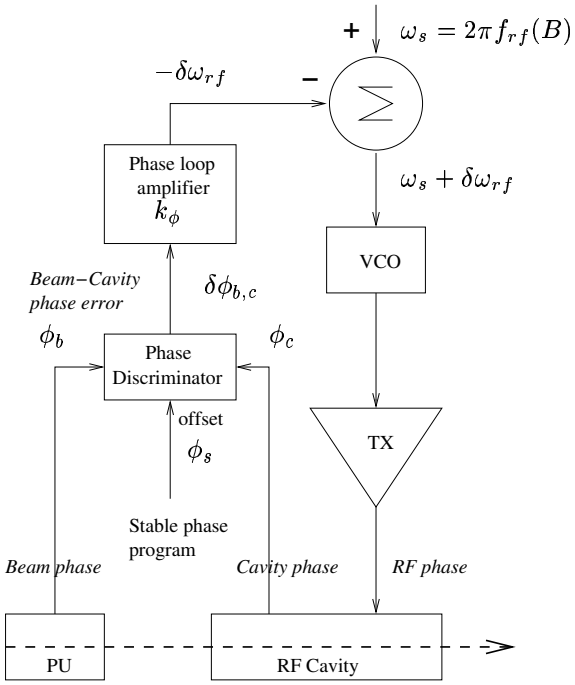

Fig. 10: Phase loop

and this provides the desired damping

$$\frac{d^2\delta\phi_{b,c}}{dt^2} + k_\phi \frac{d\delta\phi_{b,c}}{dt} + \Omega_s^2\,\delta\phi_{b,c} = 0 \ . \tag{39}$$

Remarks

- The stable phase ϕ_s is computed from a measurement of the RF voltage and the rate of change of the magnetic field (stable phase programme (7)) and fed as an offset in the phase discriminator so that the range and linearity of this device are not important. (Note that the systems presented in Section 3.3 generate a signal proportional to the cosine of the phase error).
- A static error in the stable phase programme will introduce a frequency error if the phase loop amplifier is DC-coupled. To avoid this, the phase loop can be AC-coupled. This method is used in the PS accelerator at CERN. It is explained in detail in Ref. [12].
- The phase of the RF must change by 180° at transition. The stable phase programme jumps from ϕ_s^- to $\phi_s^+ = \pi - \phi_s^-$.

- As already mentioned, the components at nf_{rev} in the phase error signal $\delta\phi_{b,c}$ must be carefully filtered out to avoid exciting coupled bunch instabilities.
- The poles of the closed-loop transfer function are

$$p_{\pm} = -\frac{k_\phi}{2} \pm \frac{k_\phi}{2}\sqrt{1 - \left(\frac{2\Omega_s}{k_\phi}\right)^2} \quad . \tag{40}$$

  For small phase loop gain $k_\phi < 2\Omega_s$ we have two complex conjugate poles. The impulse response is a damped sine wave. For $k_\phi = 2\Omega_s$ the two poles merge on the real axis. The system is critically damped and no oscillatory behaviour occurs. For larger gains $k_\phi > 2\Omega_s$ one pole moves to a large negative value on the real axis (i.e. very fast damping) but the other pole moves to the origin. The system becomes unstable at very low frequency. It presents the behaviour of an integrator. *With a phase loop alone one cannot increase k_ϕ much above critical damping*. But this limitation will disappear when we combine the phase loop with another loop.
- With a phase loop the RF noise is less likely to blow up the emittance (see Section 5.1).

4.2 Controlling the radial position: the radial loop

Motivation: In large machines the transverse aperture is usually very small. In the CERN SPS for example ($R = 1100$ m) we accept an average orbit displacement of a few millimetres only ($\frac{\delta R}{R} = 10^{-6}$). An error in the RF frequency will cause a displacement of the orbit given by Eq. (80)

$$\frac{\delta R}{R} = \frac{\gamma^2}{\gamma_t^2 - \gamma^2}\frac{\delta f_{rf}}{f_{rf}} \quad . \tag{41}$$

The required precision for the RF frequency therefore depends on the energy. It is infinite at transition! As a consequence it is difficult to control the beam radial position if the RF frequency is adjusted from a measurement of the B field only (Eq. 29). With a radial loop the required precision can be much relaxed.
Method: Figure 11 shows the radial feedback loop. We measure the radial displacement of the beam and correct the RF frequency accordingly.

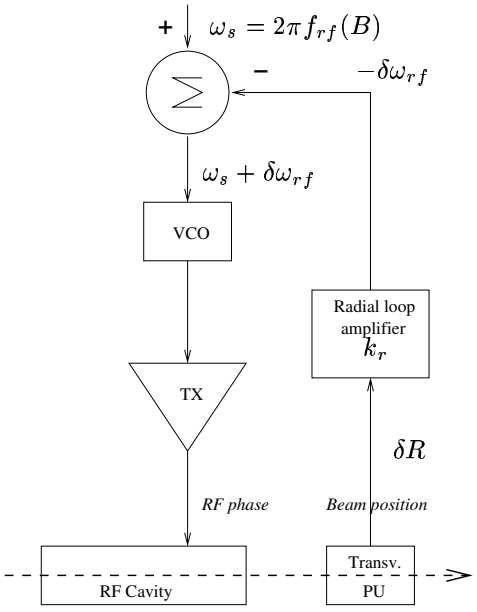

Fig. 11: Radial loop

The radial displacement δR is proportional to the momentum deviation δp, Eq. (81)

$$\delta R = \frac{R_0}{p_s \gamma_t^2} \delta p \tag{42}$$

With the above equation we can rewrite Eq. (12)

$$\frac{d^2}{dt^2} \delta R + \Omega_s^2 \, \delta R = \frac{qV cos\,(\phi_s)}{2\pi p_s \gamma_t^2} \delta \omega_{rf} = a \, \delta \omega_{rf} \tag{43}$$

with

$$a = \frac{qV cos\,(\phi_s)}{2\pi p_s \gamma_t^2} \tag{44}$$

With the feedback loop ($\delta \omega_{rf} = -k_r \, \delta R$) the equation of motion becomes

$$\frac{d^2}{dt^2} \delta R + \Omega_s^2 \, \delta R = -a k_r \, \delta R \tag{45}$$

or

$$\frac{d^2}{dt^2} \delta R + \left(\Omega_s^2 + a k_r \right) \delta R = 0 \ . \tag{46}$$

The radial loop does not provide damping since the above differential equation has no first order derivative term. It only reduces the effect of a frequency error on the radial position.

Consider a small static error ϵ_{rf} in the frequency programme $f_{rf}(B)$. This produces an error $\delta \omega_{rf} = 2\pi \epsilon_{rf}$ in the right-hand side of Eq. (43). Without the radial loop the resulting radial error would be $(2\pi a \epsilon_{rf}) / \Omega_s^2$ wher as the radial loop will reduce it to $(2\pi a \epsilon_{rf}) \, / \, (\Omega_s^2 + a k_r)$. The radial loop gain k_r cannot be made arbitrarily large, however, because the transient response of the loop is indeed changing the beam energy, and our derivation of the longitudinal dynamics assumed that the energy change per turn was small, so the momentum increment of Eq. (3) could be approximated by the continuous derivative of Eq. (4). This condition is called adiabatic evolution. The radial loop will respect this condition only if its time constant is long compared to the synchrotron period $2\pi / \Omega_s$. A classic low-level system for hadron machines will include both a fast phase loop and a slow radial loop as shown in Fig. 12. With these two loops the equation of motion now becomes

$$\frac{d^2 \delta \phi_{b,c}}{dt^2} + k_\phi \frac{d \delta \phi_{b,c}}{dt} + \left(\Omega_s^2 + a k_r \right) \delta \phi_{b,c} = 0 \ . \tag{47}$$

The poles of the closed-loop transfer function are

$$p_\pm = -\frac{k_\phi}{2} \pm \frac{k_\phi}{2} \sqrt{1 - 4 \left(\frac{\Omega_s^2 + a k_r}{k_\phi^2} \right)} \ . \tag{48}$$

If we choose $k_\phi >> \Omega_s$ and $k_\phi^2 >> a k_r$ we get

$$p_- \approx -k_\phi \tag{49}$$

$$p_+ \approx -\frac{\Omega_s^2 + a k_r}{k_\phi} \tag{50}$$

The first pole corresponds to the very fast transient defined by the phase loop gain k_ϕ. Thanks to the radial loop gain k_r the second pole can now be placed on the real axis at the desired distance from the origin. The corresponding time constant must however be long compared to the synchrotron period so that the motion remains adiabatic

$$\frac{\Omega_s^2 + a k_r}{k_\phi} < \Omega_s \ . \tag{51}$$

This places a bound on the gain of the radial loop.

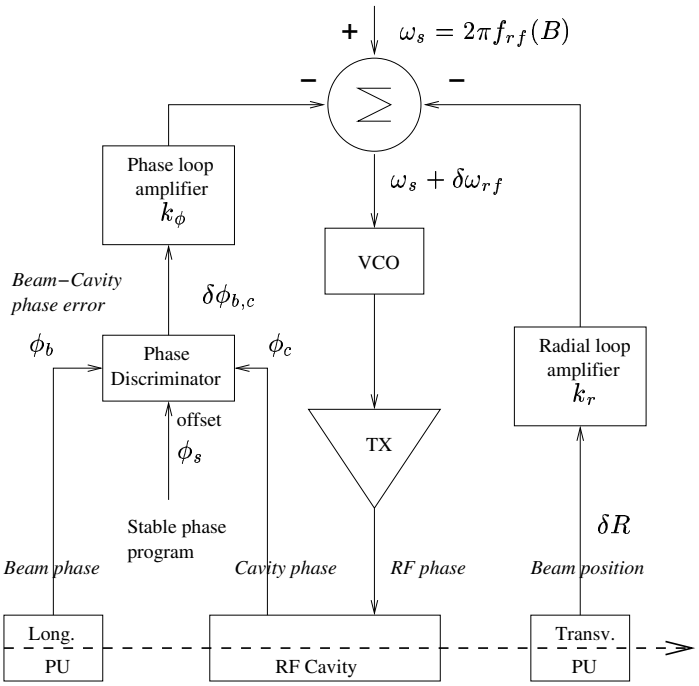

Fig. 12: Classic low-level system for hadron machines: phase loop and radial loop

Remarks

- The phase loop/radial loop tandem has a very good behaviour during transients. At injection, for example, if the beam is injected with a phase and energy error the first turn will be on an off-centred orbit and the beam will see a non-zero RF voltage. The phase loop reacts in a few turns and the RF jumps on the bunch, thereby preventing emittance blow-up. Thereafter the radial loop will slowly modify the beam energy to drive it back to the centre orbit.
- If one neglects the delays, the combination of phase loop/radial loop is unconditionally stable. A comprehensive treatment of the low-level loops in the presence of long delays can be found in Ref. [13]. Other interesting references are [14] (low-level loops with delays), [15] (application to the CERN PS in during the 1970s), and [16] (application to the CERN PS Booster).
- The gain of the radial loop amplifier must be inverted at transition because the sign of the coefficient a then changes (Eq. 43).
- With a radial loop, the noise in the loops changes the radial position and thus the beam momentum. This may be a problem when the beam is transferred to the next machine or sent to the target.
- One problem of the radial loop is that it estimates the *mean* radial position from one or two measurements at discrete points in the machine. As mentioned in Section 3.2, eventual transverse betatron oscillation and local closed orbit distortion at the pick-up location will introduce errors.

4.3 Controlling the beam frequency: the frequency loop

Motivation: The same dynamic behaviour can be achieved if the radial loop is replaced by a frequency loop. The advantage of the frequency loop is the better dynamic range and lower noise achievable with phase measurements than with radial position measurements.

Method: At constant B field the radial displacement δR is proportional to the beam frequency deviation $\delta\omega_b$ Eq. (80)

$$\frac{\delta R}{R} = \frac{\gamma^2}{\gamma_t^2 - \gamma^2}\frac{\delta\omega_b}{\omega_b} \tag{52}$$

We can thus replace the radial loop by a frequency loop as shown in Fig. 13.

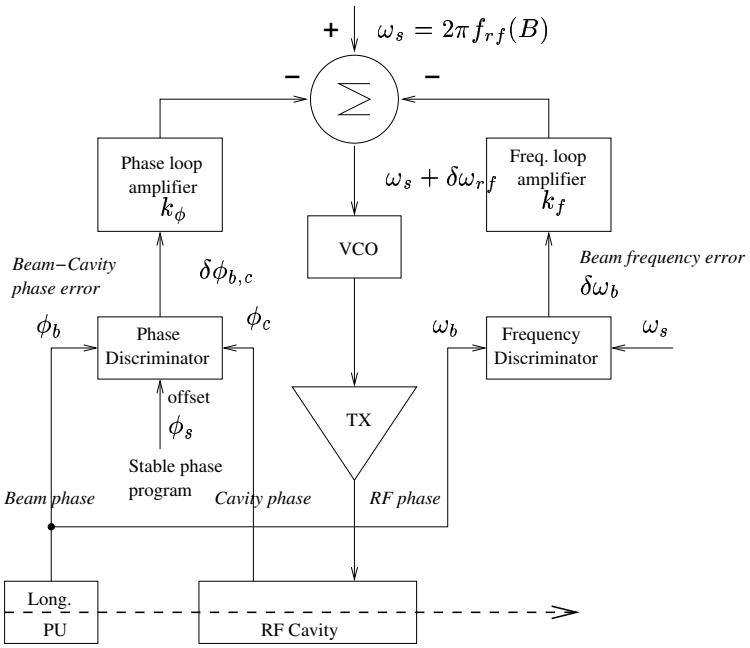

Fig. 13: Alternative low-level system for hadron machines: phase loop and frequency loop

Remark: Although the transient behaviour of the systems Figs. 12 and 13 can be made identical by varying the frequency loop gain as a function of the energy, to follow Eq. (52), there is no control of the actual radial position with the frequency loop. Beam centring is a function of the accuracy of the frequency programme $f_{rf}(B)$ only. The problem is particularly severe at transition where the beam orbit can be displaced without any change in the beam frequency (Eq. 52).[4] A variant of the system was used in the CERN SPS when it was operating as a proton–antiproton collider: the measurement of the beam frequency was replaced by a measurement of the Voltage Controlled Oscillator (VCO) frequency. The beam was injected above transition.

4.4 Controlling the beam phase: the synchronization loop

Motivation: If the transfer is of the bunch-into-bucket type, the beam in the injector must be synchronized with the RF of the receiving machine before transfer.

Method: We compare the phase of the beam with the phase of the external reference and feed the error back into the VCO after proper filtering by the synchronization loop amplifier (Fig. 14). The overall system is described by a third order differential equation. Its analysis is easier if we use Laplace transforms. Taking the transform of both sides of Eq. (37) we derive the beam transfer function $B_\phi(s)$ (dipolar motion)

$$\delta\phi_{b,c}(s) = \frac{s}{s^2 + \Omega_s^2}\delta\omega_{rf}(s) = B_\phi(s)\,\delta\omega_{rf}(s) \tag{53}$$

with

$$B_\phi(s) = \frac{s}{s^2 + \Omega_s^2}\ . \tag{54}$$

In the above equation the same symbols are used for time domain signals and for their Laplace transforms. The argument (s) identifies the transform domain. Equation (9) can also be written for the

[4] With very precise control of frequency and stable phase it is not impossible to accelerate through transition: this has been done in the acceleration of ions in the CERN SPS.

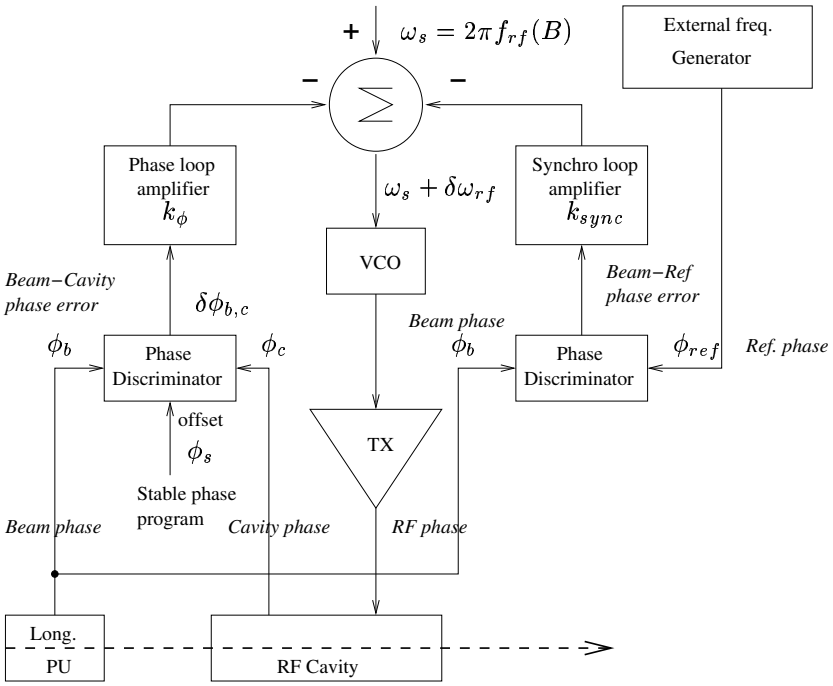

Fig. 14: Common low-level system for synchronizing two machines before transfer: phase loop and synchronization loop

beam frequency ω_b (in radian per second)

$$\frac{d\phi_{b,c}}{dt} = -\delta\omega_b + \delta\omega_{rf} \tag{55}$$

After taking Laplace transforms and rearranging the terms we get the frequency response $B_\omega(s)$ relating the beam frequency (actually its deviation with respect to the synchronous particle) to the RF frequency modulation

$$\delta\omega_b(s) = \delta\omega_{rf} - s\,\delta\phi_{b,c}(s) \tag{56}$$

$$\delta\omega_b(s) = (1 - sB_\phi(s))\,\delta\omega_{rf} = B_\omega(s)\,\delta\omega_{rf} \tag{57}$$

with

$$B_\omega(s) = \frac{\Omega_s^2}{s^2 + \Omega_s^2} \ . \tag{58}$$

We now redraw the phase and synchronization loops of Fig. 14 with the above transfer functions (Fig. 15). The beam frequency deviation $\delta\omega_b$ is integrated to give $\delta\phi_b$, that is, the beam phase minus the linear ramp at the synchronous frequency

$$\delta\phi_b = \phi_b - \omega_s t \ . \tag{59}$$

The phase loop is kept closed. We derive the open loop transfer function from the synchronization loop correction $\delta\omega_{sync}$ to the the phase of the beam $\delta\phi_b$

$$H_{ol}(s) = \frac{\delta\phi_b(s)}{\delta\omega_{sync}(s)} = \frac{1}{1 + k_\phi B_\phi(s)} B_\omega(s) \frac{1}{s} = \frac{\Omega_s^2}{s\,(s^2 + k_\phi\, s + \Omega_s^2)} \ . \tag{60}$$

The phase loop gain k_ϕ is typically much larger than Ω_s so that the open loop can be approximated by two integrators in series, i.e. 180° phase shift. $H_{ol}(j\omega)$ is plotted in Fig. 16 after multiplication by k_ϕ to render it dimensionless.

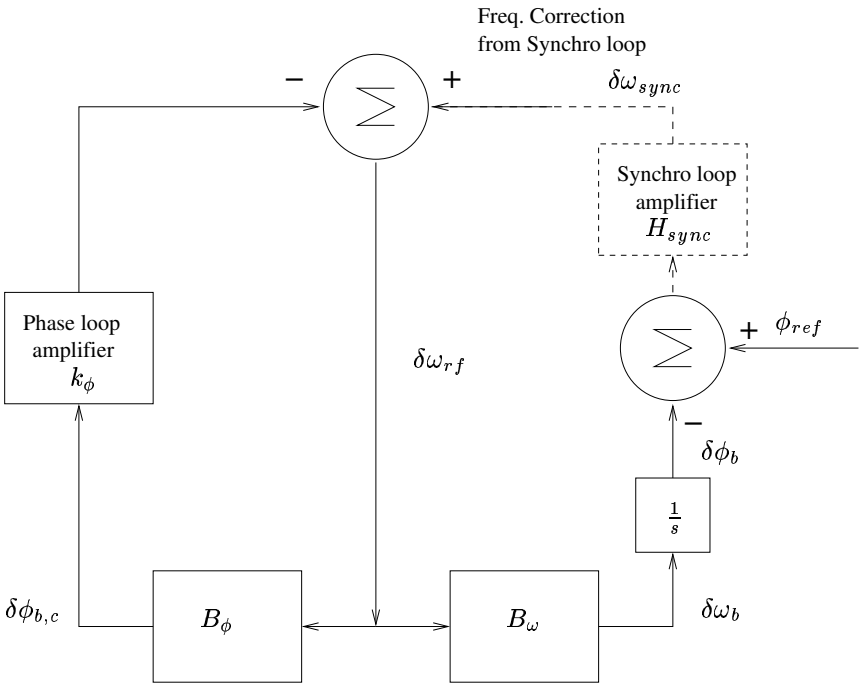

Fig. 15: Phase loop and synchronization loop in the Laplace domain

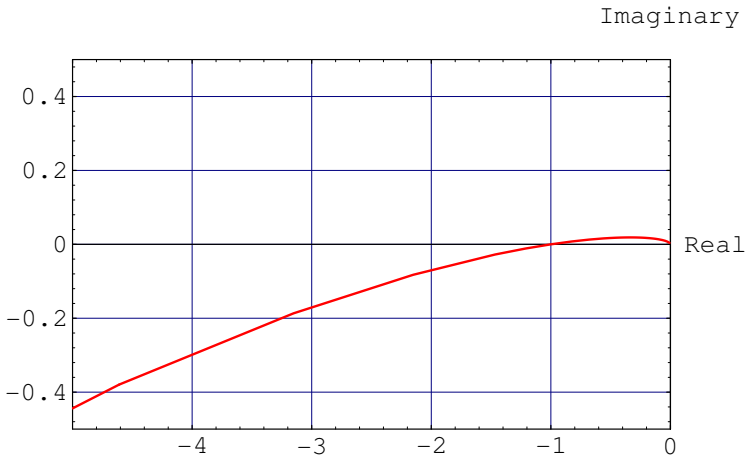

Fig. 16: Nyquist diagram of $k_\phi H_{ol}(j\omega)$ for $k_\phi = 0.6 f_{rev}$, $\Omega_s = 2\pi 200$ (rad/s). Case of the LHC proton beams in the SPS at injection ($f_{rev} = 43$ kHz).

Even with a very small gain, k_{sync}, the closed loop will be on the edge of instability. A classic indicator of stability is the phase margin, defined as the amount by which the phase of the open loop response $k_\phi H_{ol}(j\omega)$ exceeds $-180°$ when the modulus of its gain is one [17]. The phase margin should be minimum $45°$ for reasonable stability. Figure 16 shows that this condition cannot be fulfilled even for very small values of the synchronization loop gain k_{sync}. The solution is to introduce a lead compensation network $H_{sync}(s)$ in series with the open loop [17].

$$H_{sync}(s) = k_{sync}\frac{1+\alpha\tau s}{1+\tau s} \quad . \tag{61}$$

It adds a positive phase shift (dependent on the value of α), thereby increasing the phase margin. In our case the desired phase shift is $45°$, achievable with a parameter α of 7 minimum [18]. We choose $\alpha = 10$. The time constant τ adjusts the frequency ω_m at which the phase shift is maximum

$$\omega_m = \frac{1}{\tau\sqrt{\alpha}} \quad . \tag{62}$$

Using Kuo's method [18][5] we get, for a strong phase loop ($k_\phi \gg \Omega_s$)

$$\tau \approx \frac{1}{\Omega_s}\sqrt{\frac{k_\phi}{k_{sync}}}\frac{1}{\alpha^{3/4}} \quad . \tag{63}$$

The open-loop response now becomes

$$G_{ol}(s) = \frac{\Omega_s^2}{s\left(s^2 + k_\phi\, s + \Omega_s^2\right)}\frac{1+\alpha\tau s}{1+\tau s} \quad . \tag{64}$$

It is plotted in Fig. 17. With $k_{sync} = \frac{1}{4}k_\phi$ and $\alpha = 10$ the phase margin is $55°$.

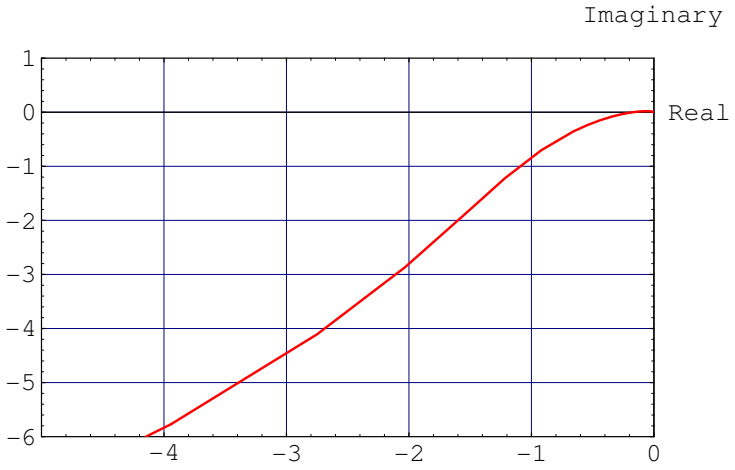

Fig. 17: Nyquist diagram of $k_\phi G_{ol}(j\omega)$ for $k_\phi = 0.6 f_{rev}$, $\Omega_s = 2\pi 200$ (rad/s) with the lead compensation network ($\alpha = 10$, $\tau = \frac{0.36}{\Omega_s}$)

Figure 18 shows the corresponding step response: Beam phase ϕ_b for a step in the reference phase ϕ_{ref}.

Remarks:

- The above design is used in the CERN SPS to accelerate the proton beam for the LHC [19],[20]. The phase loop must be much faster than the synchronization loop: in the above design its time constant[6] is 60 μs while the synchronization loop responds in a few milliseconds (Fig. 18).

[5] We choose τ such that the open loop gain, after compensation, will be 1.0 at the frequency ω_m, where the phase shift is maximum (Eq. 62).

[6] This means that it takes 60 μs to reduce a phase error at injection by a factor $1/e$.

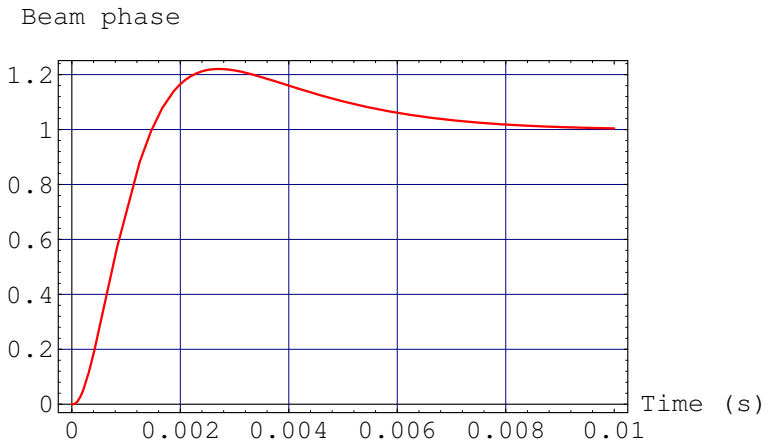

Fig. 18: Synchronization loop step response: beam phase ϕ_b for a step in the reference phase ϕ_{ref}. ($k_\phi = 0.6 f_{rev}, \Omega_s = 2\pi 200$ (rad/s), $k_{sync} = \frac{1}{4} k_\phi$, $\alpha = 10$)

- The use of a synchronization loop is common in injectors for bunch-into-bucket transfer. The external frequency generator is then the RF of the receiving machine. Synchronization scenarios comprise two steps [13]: the frequency of the injector is brought a desired offset $\Delta\omega$ from the frequency of the receiving machine (step 1). The synchronization loop is kept open and the output of the phase discriminator $(\phi_{ref} - \phi_b)$ is then a slowly-beating signal at the frequency $\Delta\omega$. The synchronization loop is closed on a zero crossing of this signal (step 2).
- A synchronization loop can also be used during acceleration if the external frequency generator implements the frequency programme $f_{rf}(B)$ Eq. (29) [19],[20]. The time constant of the lead compensation network is inversely proportional to Ω_s and must be varied during the acceleration. Acceleration with a synchronization loop is thus practical only if the synchrotron frequency does not change too much during the acceleration ramp (i.e. injection well above transition).
- One can also switch onto a synchronization loop before sending the beam to the targets. The advantage of this is that the beam energy (radial position) is precisely defined by the external frequency if the B field is assumed constant and stable. The noise and beam intensity-dependent offsets in the low-level RF will not affect the momentum of the beam delivered to the physicist, this being a weak point of the radial loop.

5 IMPLEMENTATION

5.1 The all-analog beam control

The all-analog beam control it is a straightforward implementation of the loops. The key component is the Voltage Controlled Oscillator (VCO). At RF frequencies, varactor-tuned oscillators are common. An external LC circuit (tank) sets the centre frequency and a variable capacitance diode is used to do the tuning: By varying the DC voltage applied to this diode one varies the VCO output frequency (Fig. 19).

A typical component broadly used at CERN (PS and SPS) is the MC1648 from Motorola. Its successor, the MC12149, can be tuned to oscillate at frequencies up to 1.3 GHz. Observed on a spectrum analyser the output of the VCO is not a pure line but rather a narrow lobe, whose width is caused by the phase noise. An essential figure of merit is the noise spectrum expressed in dBc/Hz as a function of the frequency offset from the carrier (Fig. 20). (One plots the ratio of the Power Spectral Density (PSD) over the power of the RF output on a logarithmic scale.)

Let us now study the effect of this noise on the beam in the presence of a phase loop.

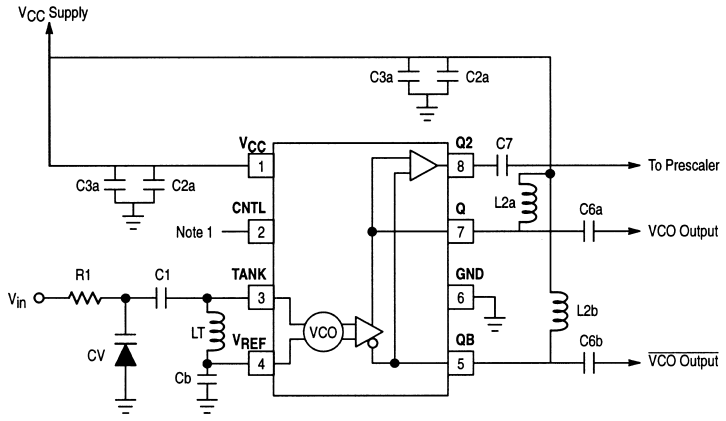

Fig. 19: Varactor-tuned oscillator (Motorola documentation)

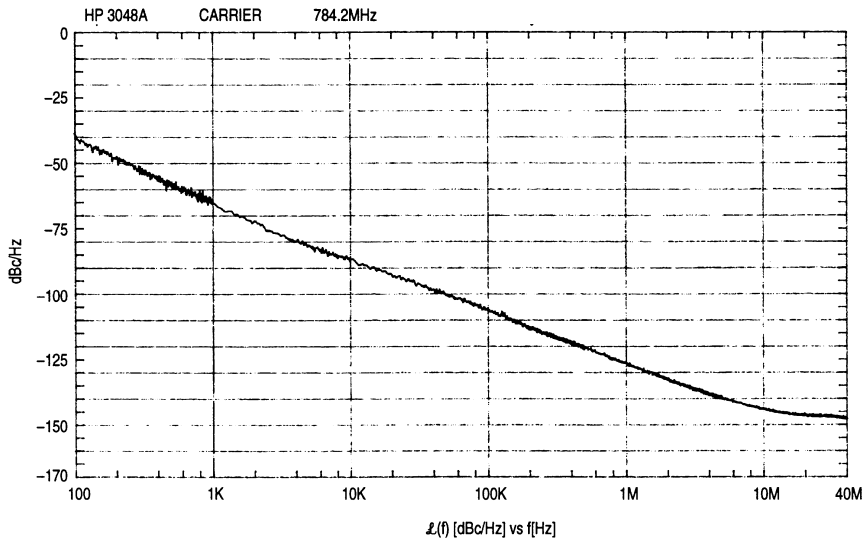

Fig. 20: Typical phase noise power spectral density $S_n(\omega)$ for MC12149 with a centre frequency at 750 MHz (Motorola documentation)

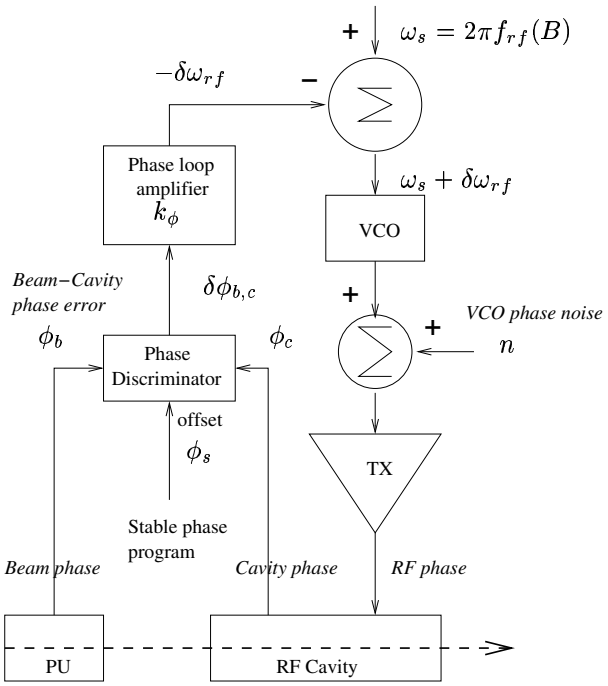

Fig. 21: Phase loop with the VCO phase noise n

The phase noise is introduced as a small random signal n added at the VCO output (Fig. 21). This noise modifies the driving term in Eq. (37). Since the RF frequency is the derivative of the RF phase the noise appears as a second derivative in the right-hand side of the equation

$$\frac{d^2\delta\phi_{b,c}}{dt^2} + \Omega_s^2\delta\phi_{b,c} = \frac{d\left(\delta\omega_{rf} + \frac{dn}{dt}\right)}{dt} = \frac{d\delta\omega_{rf}}{dt} + \frac{d^2n}{dt^2} \ . \tag{65}$$

With the phase loop closed we get

$$\frac{d^2\delta\phi_{b,c}}{dt^2} + k_\phi\frac{d\delta\phi_{b,c}}{dt} + \Omega_s^2\delta\phi_{b,c} = \frac{d^2n}{dt^2} \ . \tag{66}$$

The above equation tells us how the VCO phase noise n transforms into cavity/beam phase noise $\phi_{b,c}$. From Eq. (66) we derive the PSD $S_\phi(\omega)$ of the latter[7]

$$S_\phi(\omega) = \frac{\omega^4}{\left(\omega^2 - \Omega_s^2\right)^2 + \left(k_\phi\,\omega\right)^2}S_n(\omega) \ . \tag{67}$$

The second factor on the right-hand side is the spectrum plotted in Fig. 20. The first factor shows the effect of the phase loop. We shall call it the noise enhancement factor (Fig. 22). It is equal to zero at DC because slow drifts of the RF phase are followed by the beam and the cavity/beam phase remains zero. At very high frequencies the factor equals one. The beam does not react any more and the VCO noise is transmitted directly to the cavity/beam phase. Around the synchrotron frequency the enhancement factor depends on the phase loop gain. With $k_\phi = 0$ (no phase loop) it is infinite: the centre of charge of the bunch will thus see large RF phase errors. This will cause filamentation and will result in emittance blow-up and eventually loss of particle, as previously shown for an injection phase error (Fig. 8). As we increase the loop gain k_ϕ the factor is reduced in an increasing frequency band around the synchrotron frequency (Fig. 22).

[7] The PSD $S_y(\omega)$ of the output y of a linear system with transfer function $H(j\omega)$ is given by $S_y(\omega) = |H(j\omega)|^2 S_x(\omega)$ where $S_x(\omega)$ is the PSD of the input x [21].

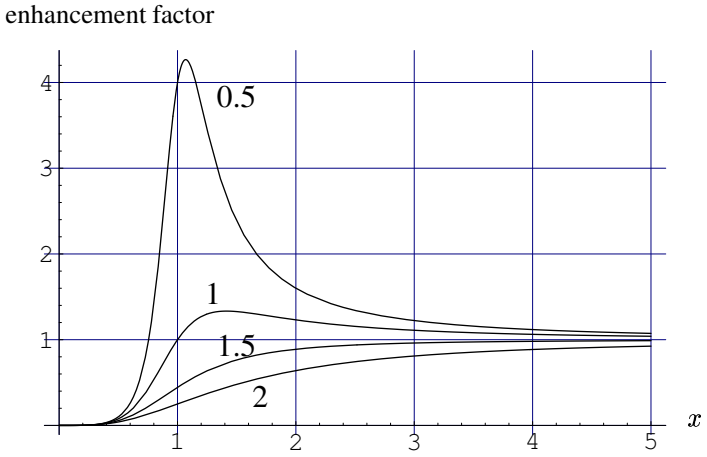

Fig. 22: Enhancement of the VCO noise: $\frac{x^4}{\left(x^2-1\right)^2+\xi^2 x^2}$ as a function of $x = \frac{\omega}{\Omega_s}$ for different values of the normalized phase loop gain $\xi = \frac{k_\phi}{\Omega_s}$ (from top trace to bottom: $\xi = 0.5, 1, 1.5, 2$)

A similar analysis can be done for the noise injected elsewhere in the beam control system: the noise in the frequency programme, for example, is injected in the adder at the top of Fig. 21. The resulting PSD of the cavity/beam phase will be given by a formula similar to Eq. (67) but the numerator will be ω^2 instead of ω^4 because of the integrator characteristic of the VCO. The phase loop will also reduce the damaging effect of this noise.

Nowadays the all-analog implementation is of limited use: the lack of precision in the analog voltage provided by the frequency programme implies poor control of the orbit since the gain of the radial loop cannot be infinite.

5.2 Analog beam control with DDS

To increase the precision of the frequency programme the analog VCO is replaced by a digital frequency synthesizer with a high resolution (i.e. many bits in the frequency word). These are called DDS, for Direct Digital Synthesizer. They present continuity in the phase of the RF output while the frequency is changing during the acceleration ramp. Figures 23 and 24 explain the DDS principle: at each clock pulse the content of the accumulator S is incremented by the digital frequency word F. The accumulator

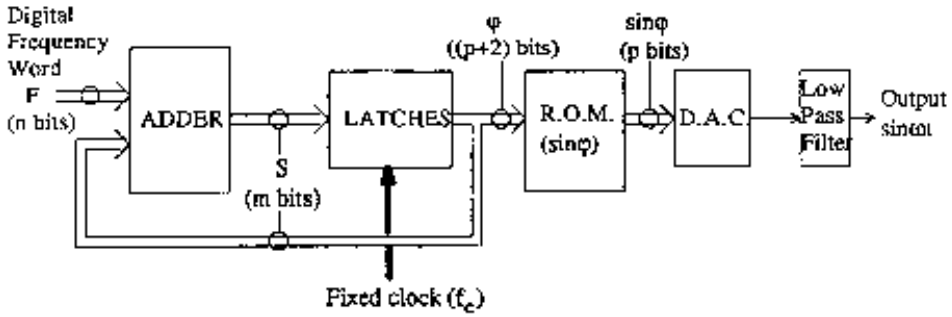

Fig. 23: Elementary block diagram for DDS. Reproduced from Ref. [22].

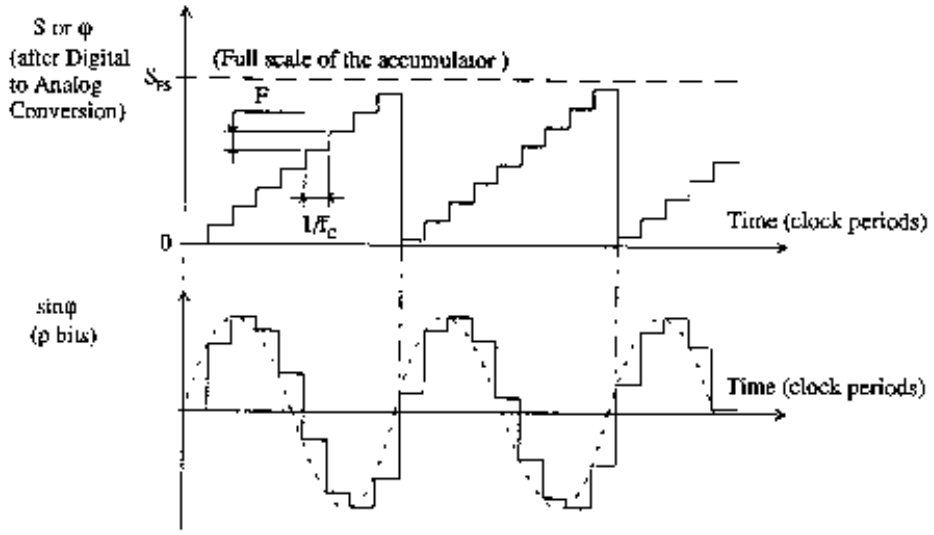

Fig. 24: Signal generation in DDS. Reproduced from Ref. [22].

regularly overflows, creating a quantized sawtooth whose frequency is proportional to F. The sawtooth is transformed into a sine wave by the Read Only Memory (ROM) and finally converted into an analog output. The frequency resolution depends on the number of bits for the control word F and the frequency range depends on the clock frequency f_c. For example, the AD9854, from Analog Devices, can be clocked at 300 MHz and has a 48-bit frequency word, thus providing a 1μHz resolution for a 100 MHz range. The noise at the output of a DDS has two components: the first comes from the division of the phase noise of the clock. It is similar to the noise of an analog VCO but will typically be very small because it is easy to get high spectral purity from a clock at a fixed frequency. The second component comes from the non-linearity of the digital quantization: this produces spurious lines whose amplitude varies in a complex fashion when changing the output frequency. Figure 25 shows the corresponding spectrum. The Spurious Free Dynamic Range (SFDR) is the component's important figure of merit: it measures the minimal guaranteed attenuation of the spurious lines with respect to the desired output signal.

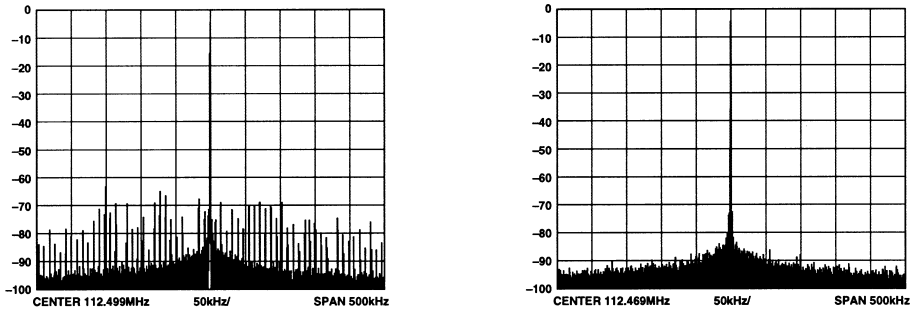

Fig. 25: Typical spectrum of the output of a DDS in a 500 kHz span centred on the carrier (0 dBm). Left: carrier at 112.499 MHz; right: carrier at 112.469 MHz. Notice the severe degradation of the spectrum for a small change in output frequency. The Spurious Free Dynamic Range (SFDR) in this 500 kHz band is here about 65 dB (Analog Devices documentation).

5.3 The digital beam control

In order to take advantage of the digital precision of the DDS, the low frequency part of the low-level loops should also be digital. Only the fast acquisition part remains analog. Figure 26 shows the beam control system used in the CERN PS [11]. The output of the Phase Loop Amplifier (PLA) is digitized by a 10 MS/s (10^7 samples per second) 12-bit ADC and added to the Digital Frequency Program (DFP) output in the Digital Loop Processor (DLP). The digitally generated frequency is sufficiently accurate to centre the beam in the vacuum chamber so there is no need for a radial loop. Correction of the frequency programme is achieved with the Digital Recorder (DR), which reproduces the correction memorized during a reference acceleration where the beam was accurately centred. This correction is added in the Digital Arithmetic Unit (DAU).[8] In this design the PLA is analog. One could also digitize the phase error

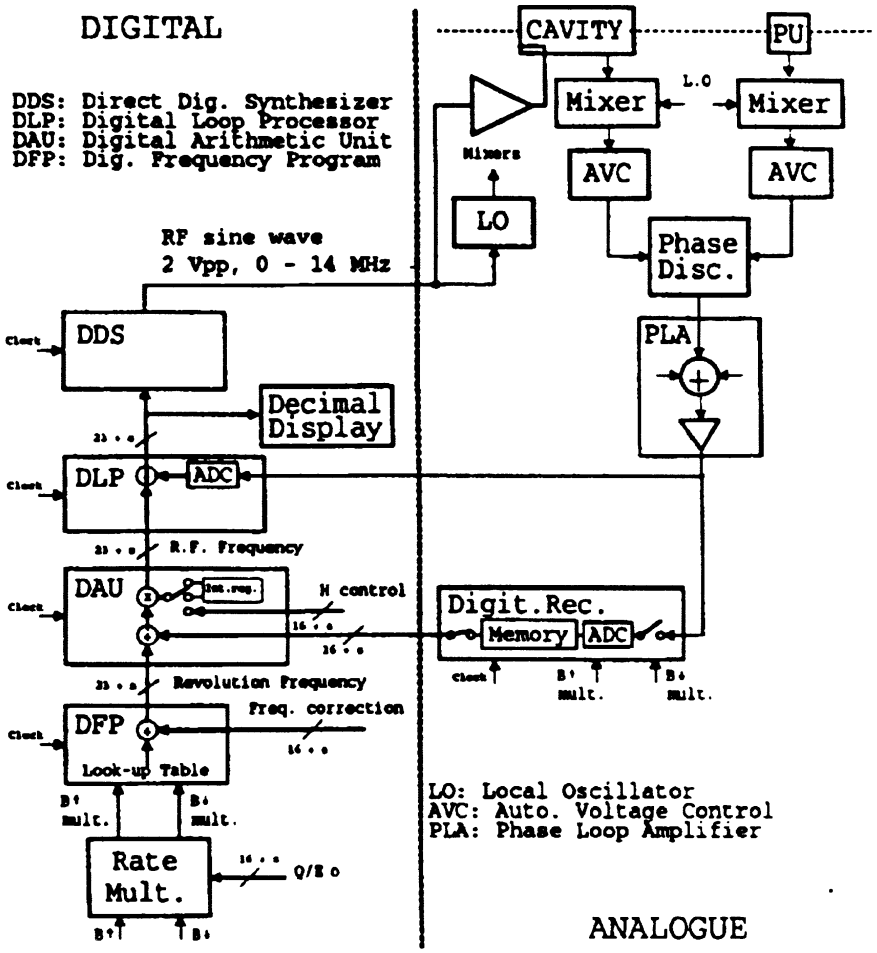

Fig. 26: Digital beam control system used in the CERN PS (reproduced from Ref. [11])

at the output of the phase discriminator and implement the low frequency part of the phase loop in digital [24].

[8] Performances were, however, much more reproducible with the radial loop in service. At present, this is the case with most beams accelerated in the CERN PS [23].

5.4 State variable and DSP implementation

We started our analysis with the description of the beam motion using a second order differential equation (Eq. 11). Alternatively we can keep the two first order differential equations. Let us use the variables $(\delta\phi, \delta R)$[9]. From Eqs. (9) and (80) we get

$$\frac{d}{dt}\delta\phi = -\frac{h\beta_s c}{R_0^2}\left(\frac{\gamma_t^2 - \gamma^2}{\gamma^2}\right)\delta R + \delta\omega_{rf} = b\,\delta R + \delta\omega_{rf} \tag{68}$$

with

$$b = -\frac{h\beta_s c}{R_0^2}\left(\frac{\gamma_t^2 - \gamma^2}{\gamma^2}\right) \quad . \tag{69}$$

and from Eqs. (8) and (81)

$$\frac{d}{dt}\delta R = \frac{qV\cos(\phi_s)}{2\pi p_s \gamma_t^2}\delta\phi = a\,\delta\phi \tag{70}$$

with

$$a = \frac{qV\cos(\phi_s)}{2\pi p_s \gamma_t^2} \quad . \tag{71}$$

The state of the beam is now given by the vector $(\delta\phi, \delta R)$. Its time evolution follows the equations

$$\frac{d}{dt}\begin{pmatrix} \delta\phi \\ \delta R \end{pmatrix} = \begin{pmatrix} 0 & b \\ a & 0 \end{pmatrix}\begin{pmatrix} \delta\phi \\ \delta R \end{pmatrix} + \begin{pmatrix} 1 \\ 0 \end{pmatrix}\delta\omega_{rf} \tag{72}$$

The coefficients of the square matrix vary slowly with time since a and b vary during the acceleration. Of course $a.b = -\Omega_s^2$. The phase loop and radial loop feedback can now be introduced

$$\delta\omega_{rf} = -\begin{pmatrix} k_\phi & k_r \end{pmatrix}\begin{pmatrix} \delta\phi \\ \delta R \end{pmatrix} \tag{73}$$

and the equations become

$$\frac{d}{dt}\begin{pmatrix} \delta\phi \\ \delta R \end{pmatrix} = \begin{pmatrix} -k_\phi & b - k_r \\ a & 0 \end{pmatrix}\begin{pmatrix} \delta\phi \\ \delta R \end{pmatrix} \quad . \tag{74}$$

The transient behaviour of the system is determined by the eigenvalues λ of the above matrix. The characteristic equation is

$$\lambda^2 + k_\phi\lambda + (ak_r - ab) = 0 \ . \tag{75}$$

The eigenvalues are identical to the poles of the second order differential equation (47). We can choose the eigenvalues and compute the gain coefficients k_ϕ and k_r during the ramp in order to keep the same loop behaviour through the cycle. This method is called pole placement in control theory [17] : one first chooses a *cost function* that measures the error between the desired and actual responses of the system in presence of a perturbation. The optimal positions of the poles minimize this cost function. The use of state variable is somewhat academic for the phase loop/radial loop system. For more complex loops (synchronization loop with lead compensation for example) a set of four first order differential equations is required. Pole placement with the above formalism should then bring a more exact derivation of the optimal values of the gains than the Nyquist analysis presented in Section 4.4. The design of a beam control using state variables was first proposed at BNL for the AGS [25].

To implement pole placement we need a processor that adjusts the feedback gains during acceleration. Nowadays this can easily be done using a Digital Signal Processor (DSP). A DSP is a microprocessor optimized for fast-floating point operations. The ADSP-2106x from Analog Devices and the TMS320C6x from Texas Instruments are used in particle accelerators. Figure 27 shows the hardware

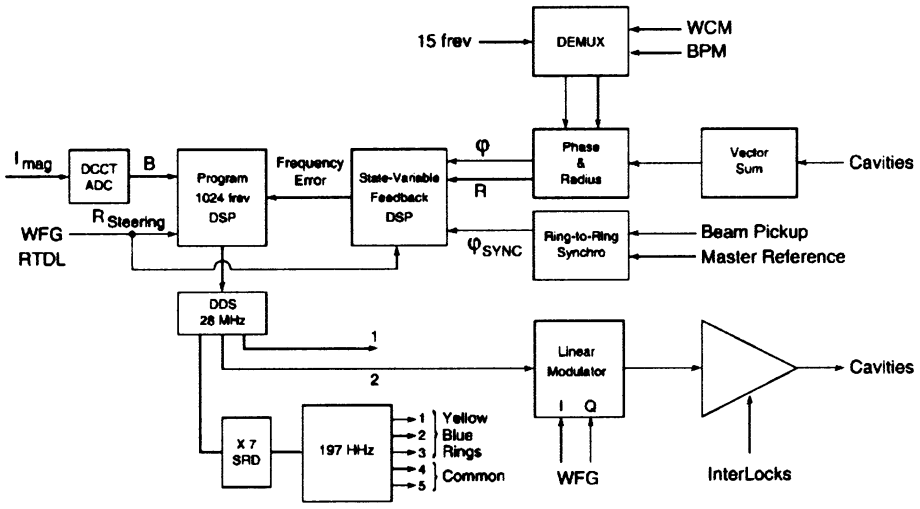

Fig. 27: Beam control system with DSP used at Fermilab for the RHIC (reproduced from Ref. [26])

used at BNL for the Relativistic Heavy Ion Collider (RHIC) [26]. One DSP computes the frequency (frequency programme) from a measurement of the B field (in fact the magnet current). It also receives a correction called the radial steering. The output is a 32-bit word providing 6 mHz resolution at 28 MHz. A second DSP, called the State-Variable Feedback DSP in the figure, implements the feedback loops. The beam phase and radius are measured once per turn (every 12 μs). The feedback gains are recomputed 200 times during the 74 s acceleration ramp. The output is the frequency error added to the DDS control word. The loops implemented by the DSP can be switched on and off at will. This is simply programmed as a C-language if/then statement. The phase loop is normally closed with either the radial loop (during acceleration) or the synchronization loop (before colliding) [26]. A similar system is in use in the Fermilab main ring and Tevatron [27].

6 ANNEXE

6.1 Differential relations

Among the four variables B, p, R, f only two can be chosen independently. The other two are then functions of these. Differential relations describe the variations of any three of these around a valid working point [3],[4] :

$$\frac{\delta p}{p} = \gamma_t^2 \frac{\delta R}{R} + \frac{\delta B}{B} \tag{76}$$

$$\frac{\delta p}{p} = \gamma^2 \frac{\delta f}{f} + \gamma^2 \frac{\delta R}{R} \tag{77}$$

$$\frac{\delta B}{B} = \gamma_t^2 \frac{\delta f}{f} + \frac{\gamma^2 - \gamma_t^2}{\gamma^2} \frac{\delta p}{p} \tag{78}$$

$$\frac{\delta B}{B} = \gamma^2 \frac{\delta f}{f} + \left(\gamma^2 - \gamma_t^2\right) \frac{\delta R}{R} \tag{79}$$

For example, from Eq. (79) we derive that, at B constant, an error in the RF frequency creates a radial position error

$$\frac{\delta R}{R} = \frac{\gamma^2}{\gamma_t^2 - \gamma^2} \frac{\delta f}{f} \quad . \tag{80}$$

[9] To simplify the notations the subscripts b, c are dropped in this section so that $\delta\phi$ now represents $\delta\phi_{b,c}$.

From Eq. (76) we can relate the radial displacement to the momentum deviation at B constant

$$\frac{\delta R}{R} = \frac{1}{\gamma_t^2}\frac{\delta p}{p} \ . \tag{81}$$

The slippage factor η is defined as the opposite of the ratio of the relative frequency deviation to the relative momentum deviation at constant B. From Eq. (78) we get

$$\eta = -\frac{\frac{\delta f}{f}}{\frac{\delta p}{p}} = \frac{1}{\gamma_t^2} - \frac{1}{\gamma^2} \ . \tag{82}$$

6.2 Notation

ϕ_s the stable phase.

ϕ_c the phase of the RF in the cavity.

ϕ the phase of the RF in the cavity when the particle crosses it.

$\delta\phi = \phi - \phi_s$.

$\hat{\phi}$ the phase of the RF in the cavity when the centre-of-charge of the bunch crosses it.

ϕ_b the phase of the beam = the phase-of-the Fourier component of the beam current at the RF frequency.

$\phi_{b,c}$ cavity/beam phase. ($\phi_{b,c} = \phi_c - \phi_b + \pi/2$).

$\delta\phi_{b,c}$ cavity/beam phase minus the stable phase. ($\delta\phi_{b,c} = \phi_c - \phi_b + \pi/2 - \phi_s$).

Ω_s the synchrotron frequency in radian/s (Eq. 13).

ω_{rf} the RF frequency in radian/s. ($\omega_{rf} = \frac{d\phi_c}{dt}$).

ω_s the synchronous frequency in radian/s = the RF frequency that keeps the beam on the centre orbit. It is a function of the B field: $\omega_s = 2\pi f_{rf}(B)$ with $f_{rf}(B)$ given by Eq. (29).

$\delta\omega_{rf}$ a small modulation of the RF frequency around the synchronous frequency. $\delta\omega_{rf} = \omega_{rf} - \omega_s$.

ω_b the beam frequency = $2\pi h$ times the revolution frequency ($\omega_b = \frac{d\phi_b}{dt}$).

$\delta\omega_b$ a small modulation of the beam frequency around the synchronous frequency. $\delta\omega_b = \omega_b - \omega_s = \frac{d\,\delta\phi_b}{dt}$.

$\delta\phi_b$ the deviation of the beam phase from the linear ramp at the synchronous frequency. ($\delta\phi_b = \phi_b - \omega_s t$).

REFERENCES

[1] John J. Livingood, *Principles of Cyclic Particle Accelerators* (D. Van Nostrand, Princeton, NJ, 1961).

[2] H. Bruck, Accélérateurs circulaires de particules, [Circular Particle Accelerators] (Bibliothèque des Sciences et Techniques Nucléaires, Paris, 1966).

[3] L. Rinolfi, Longitudinal beam dynamics, Application to synchrotron, CERN/PS 2000-008 (LP), course given at the Joint Universities Accelerator School (JUAS), 26 April 2000.

[4] C. Bovet, R. Gouiran, I. Gumowski, K.H. Reich, A selection of formulae and data useful for the design of A.G. synchrotrons, CERN/MPS-SI/Int. DL/70/4 (1970).

[5] E. Regenstreif, Le synchrotron à protons du CERN (1ère partie, CERN 58-6 a 1958).

[6] A. Schnase, Cavities with a swing, CAS, Seeheim, 8–16 May 2000, these proceedings.

[7] J. Le Duff, High-frequency non-ferrite cavities, CAS, Seeheim, 8–16 May 2000, these proceedings.

[8] C. Boccard, CERN SL/BI, private communication.

[9] D. Cocq, CERN SL/BI, private communication.

[10] J.M. Brennan, RF beam control for the AGS booster, Brookhaven Natl. Lab., BNL-52438 (1994).

[11] F. Blas, J. Boucheron, B.J. Evans, R. Garoby, G.C. Schneider, J.P. Terrier, J.L. Vallet, Digital beam controls for synchrotrons and storage rings in the CERN PS complex, CERN/PS 94-24 (RF), presented EPAC London, 1994.

[12] R. Garoby, Low level RF and feedback, Proc. Joint US–CERN–Japan International School, Frontiers of accelerator technology, Tsukuba, 1996.

[13] S. Koscielniak, RF systems aspects of longitudinal beam control (in the low current regime), AIP conference proceedings 249 (AIP, 1992) Vol. 1.

[14] W. Schnell, Equivalent circuit analysis of phase-lock beam control systems, CERN 68-27 (1968).

[15] D. Boussard, Une présentation élémentaire du système Beam Control du PS [An elementary presentation of the PS Beam Control System], MPS/SR/Note/73-10 (1973).

[16] G.C. Schneider, RF beam control and stability for newcomers, CERN/PS 90-59 (RF) (1990).

[17] Gene F. Franklin, J. David Powell, Abbas Emami-Naeini, *Feedback Control of Dynamic Systems*, (Addison-Wesley, Reading, MA, 1994).

[18] J.-Ch. Gille, P. Decaulne, M. Pélegrin,*Théorie et calcul des asservissements Linéaires*, [Theory and Calculation of Linear Servo Control] (Dunod, Paris 1987).

[19] P. Baudrenghien, T. Linnecar, D. Stellfeld, U. Wehrle, SPS beams for LHC: RF beam control to minimise rephasing in the SPS, CERN-SL-98-027-RF, presented at EPAC, Stockholm 1998.

[20] P. Baudrenghien, Beam control for protons and ions, CERN-OPEN-99-077 (1999), presented at the 9th LEP-SPS Performance Workshop, Chamonix 1999, CERN-SL-99-007-DI.

[21] A. Papoulis, *Probability, Random Variables and Stochastic Processes* (McGraw-Hill, New York, 1965).

[22] R. Garoby, Low level RF building Blocks, RF Engineering for Particle Accelerator, Cern Accelerator School, Exeter College, 1991.

[23] R. Garoby, CERN PS, private communication.

[24] L.K. Mestha, V. Brouk, R.C. Webber, J. Mangino, T. Uher, A digital beam phase loop for the low energy booster, presented at PAC, Washington, DC, 1993.

[25] E. Onillon, J.M. Brennan, The new BNL AGS phase, radial and synchronisation loops, presented at EPAC, Sitges, 1996.

[26] J.M. Brennan, A. Campbell, J. DeLong, T. Hayes, E. Onillon, J. Rose, K. Vetter, RF beam control system for the Brookhaven relativistic heavy ion collider RHIC, presented at EPAC, Stockholm, 1998.

[27] B.E. Chase, B. Barnes, K. Meisner, Digital low level RF systems for Fermilab main ring and Tevatron, presented at PAC, Vancouver, 1997.